

Power Law and Composite Power Law Friction Factor Correlations for Laminar and Turbulent Gas–Liquid Flow in Horizontal Pipelines

F. García and R. García

School of Mechanical Engineering and Fluid Mechanics Institute,
Central University of Venezuela, Caracas 1051, Venezuela

J. C. Padrino, C. Mata and J. L. Trallero
PDVSA–Intevep, Los Teques 1201, Venezuela

D. D. Joseph

Department of Aerospace Engineering and Mechanics,
University of Minnesota, Minneapolis, MN 55455
September 2002

Abstract

Data from 2435 gas–liquid flow experiments in horizontal pipelines, taken from different sources, including new data for heavy oil from PDVSA–Intevep are compiled and processed for power law and composite power law friction factor correlations. To our knowledge this is the largest database so far published in literature; it includes the widest range of operational conditions and fluid properties for two–phase friction factor correlations. Separate power laws for laminar and turbulent flows are obtained for all flows in the database and also for flows sorted by flow pattern. Composite analytical expressions for the friction factor covering both laminar and turbulent flows are obtained by fitting the transition region between laminar and turbulent flow with logistic dose curves. Logistic dose curves lead to rational fractions of power laws which reduce to the power laws for laminar flow when the Reynolds number is low and to turbulent flow when the Reynolds number is large. The Reynolds number appropriate for gas–liquid flows in horizontal pipes is based on the mixture velocity and the liquid kinematic viscosity. The definition of the Fanning friction factor for gas–liquid flow used in this study is based on the mixture velocity and density. Error estimates for the predicted versus measured friction factor together with standard deviation for each correlation are presented. The correlations in this study are compared with previous correlations and mechanistic models most commonly used for gas–liquid flow in pipelines. Since different authors use different definitions for friction factors and Reynolds numbers, comparisons of the predicted pressure drop for each

and every data point in the database are presented. Our correlations predict the pressure drop with much greater accuracy than those presented by previous authors.

1. Introduction

The problem confronted in this study is how to predict the pressure drop in a horizontal pipeline. This problem is of great interest in many industries, especially in the oil industry. The approach taken in this work is based on recent applications of processing data from experiments (real or numerical) for power laws (Joseph, 2001; Patankar *et al.*, 2001a; Patankar *et al.*, 2001b; Patankar *et al.*, 2002; Wang *et al.*, 2002; Pan *et al.*, 2002; Viana *et al.*, 2002; Mata *et al.*; 2002).

Data from 2435 experiments, taken from different sources, have been compiled and processed. The data processed in this work include most of the data published in the prior literature plus new unpublished, and data for gas and heavy oil from PDVSA–Intevep.

Dimensionless pressure gradients are usually expressed as friction factors. The relation between pressure gradient and mass flux is expressed in dimensionless form as a relation between the friction factor and Reynolds number. In the engineering literature, one finds such plots of fluid response of one single fluid (one–phase) in the celebrated Moody diagram. The pipe roughness is an important factor in the Moody diagram; for turbulent flow in smooth pipes the data may be fit to the well-known power law of Blasius for which the friction factor increases with 0.25 power of the Reynolds number. The Moody diagram may be partitioned into the three regions: laminar, transition and turbulent.

Here, we construct ‘Moody diagrams’ for gas–liquid flows in horizontal pipelines in terms of a mixture Fanning friction factor and mixture Reynolds number selected to reduce the scatter in the data. The data is processed for power laws and a composite expression is found as a rational fraction of power laws which reduces to a ‘laminar’ power law for low Reynolds numbers and a ‘turbulent’ Blasius like expression for large Reynolds numbers. We find that pipe roughness does not have a major effect on turbulent gas–liquid flow; the effects of interacting phases appear to dominate the effects of wall roughness.

It is well known that the pressure gradient depends on the flow type and prediction of the friction for each flow type can be found in the literature. Here, we depart from the path laid down by previous authors by creating composite correlations for each flow type and also for all the data without sorting according to flow type. Of course, the correlations for separate flow patterns

are more accurate but possibly less useful than those for which previous knowledge of actual flow pattern is not required. A correlation for which a flow pattern is not specified is exactly what is needed in a field situation in which the flow patterns are not known.

The accuracy of the correlations developed in this paper is evaluated in two ways; by comparing predictions with the data from which the predictions are derived and by comparing the predictions of our correlations with predictions of other authors in the literature. The internal evaluation is carried out by looking at the spread of the data around the predicted friction factor. The standard deviation is a measure of the spread.

The comparison of our correlations with the literature is not conveniently carried in the friction factor vs. Reynolds number frame because different authors use different definitions of these quantities. An unambiguous comparison is constructed by comparing predicted pressure gradients against the experiments in our database. We compared our predicted pressure gradients with those obtained from the correlations of Dukler *et al.* (1964), Beggs and Brill (1973) and Ortega *et al.* (2001) as well as with the predictions of the mechanistic models of Xiao *et al.* (1990), of Ouyang (1998) and of Padrino *et al.* (2002). Ouyang's models are for horizontal wells which reduce to pipelines when the inflow from reservoir is put to zero.

A comprehensive performance comparison between different models and correlations is achieved by means of the so-called modified relative performance factor (PF) proposed in this study. The performance factor is a statistical measure which allows models and correlations to be ranked for accuracy.

2. Dimensionless Parameters

Due to the complexity of multiphase flow systems, it is not possible to obtain the governing dimensionless groups uniquely; various possibilities exist. For instance, Dukler *et al.* (1964) use one set, Beggs and Brill (1973) another set, Mata *et al.* (2002) another set and so on. In the present work, various combinations of dimensionless parameters were tried and judged by their success in reducing the root mean square percent relative error between the correlated and experimental values. The dimensionless parameters introduced by Mata *et al.* (2002) in a work on pressure drops in a flexible tube designed to model terrain variation is closely allied to this study and those dimensionless groups were found also to work best in our study.

The Fanning friction factor for the gas–liquid mixture is defined as:

$$f_M = \frac{(\Delta p / L)D}{2\rho_M U_M^2} \quad (1)$$

where the pressure drop per unit length ($\Delta p / L$) is related to the wall shear stress $\tau_w = (D\Delta p / 4L)$, D is the pipe diameter, $U_M = U_{SG} + U_{SL}$ is the mixture velocity which is defined in terms of the superficial gas velocity ($U_{SG} = 4Q_G / \pi D^2$) and the superficial liquid velocity ($U_{SL} = 4Q_L / \pi D^2$). Q_G and Q_L are the gas and liquid flow rates, respectively. The mixture density

$$\rho_M = \rho_L \lambda_L + \rho_G (1 - \lambda_L) \quad (2)$$

is a special kind of composite density weighted by the flow rate fraction, where λ_L is the liquid flow rate fraction.

$$\lambda_L = \frac{Q_L}{Q_L + Q_G} \quad (3)$$

The mixture Fanning friction factor f_M is correlated with a mixture Reynolds number defined by

$$\text{Re} = \frac{U_M D}{\nu_L} \quad (4)$$

where $\nu_L = \mu_L / \rho_L$ is the kinematic viscosity of the liquid; this definition acknowledges that the frictional resistance of the mixture is due mainly to the liquid.

The mixture friction factor f_M and the mixture Reynolds number Re definitions are greatly important in order to develop an appropriate correlation of the experimental data.

3. Universal (all flow patterns) composite (all Reynolds numbers) correlation for gas–liquid friction factors

Gas flow rate Q_G , liquid flow rate Q_L and differential pressure Δp measurements corresponding to 2435 experimental points taken from Intevep's databank, the Stanford multiphase flow database (SMFD), and the database of the Tulsa University fluid flow projects (TUFFP) for gas–liquid flow in horizontal pipes used in this study. This data is summarized tables 1 – 3. The columns in the tables are self explanatory except that 'points' means the number of experiments, ε / D is the average size of pipe wall roughness over pipe diameter, FP

means ‘flow pattern’ and AN, DB, SL, SS and SW stand annular, dispersed bubble, slug, stratified smooth and stratified wavy flow, respectively.

Table 1. Intevep data

Source	Points	Fluids	μ_L [cP]	U_{SL} [m/s]	U_{SG} [m/s]	D [m]	ε/D	FP
Cabello <i>et al.</i> (2001)	26+9*	Air-Kerosene	1	0.11 – 4.52	0.77 – 45.65	0.0508	0	AN
								DB
								SL
								SL-AN
								SL-DB
Mata <i>et al.</i> (2002)	31	Air-Oil	100	0.11 – 1.49	0.06 – 3.43	0.0254	0	SL
Rivero <i>et al.</i> (1995)	74	Air-Water	1 – 200	0.02 – 0.19	0.61 – 11.89	0.0508	0	SW
		Air-Oil						
Ortega <i>et al.</i> (2000)	50+20*	Air-Oil	500	0.10 – 2.77	0.02 – 38.24	0.0508	0	AN
								DB
								SL
								SS
								SW
								SL-AN
								SL-DB
SS-SL								
SW-AN								
Ortega <i>et al.</i> (2001)	35+12*	Air-Oil	1200	0.01 – 0.80	0.23 – 24.39	0.0508	0	AN
								SL
								SW
								SL-AN
								SW-AN
Pereyra <i>et al.</i> (2001)**	94	Gas-HL	8 – 400	2.69 – 0.58	0.26 – 12.91	0.0779	$5.9 \cdot 10^{-4}$	SL

* Transitions points, ** The live oil viscosity is reported

Table 2. Stanford data

Source	Points	Fluids	μ_L [cP]	U_{SL} [m/s]	U_{SG} [m/s]	D [m]	ϵ/D	FP
Alves (1954)	28	Air–Oil	80	0.02 – 1.78	0.12 – 13.16	0.0266	$1.7 \cdot 10^{-3}$	AN
								SL
								SW
Govier and Omer (1962)	57	Air–Water	1	0003 – 1.53	0.05 – 16.57	0.0261	0	AN
								SL
								SS
								SW
Agrawal (1971)	19	Air–Oil	5	0.01 – 0.06	0.11 – 6.16	0.0258	0	SS
Yu (1972)	15	Air–Oil	5	0.10 – 0.32	0.07 – 0.62	0.0258	0	SL
Eaton (1966)	51	Gas–Water	1	0.04 – 2.24	0.28 – 22.42	0.0508	$8.0 \cdot 10^{-4}$	SL
								SS
								SW
Mattar (1973)	8	Air–Oil	5	0.31 – 1.55	0.30 – 7.83	0.0258	0	SL
Aziz <i>et al.</i> (1974)	128	Air–Oil	5	0.03 – 1.68	0.02 – 3.75	0.0258	0	DB
								SL
Companies*	141	Air–HL	3 – 19	0.07 – 6.26	0.32 – 63.44	0.0232	$6.5 \cdot 10^{-5}$	AN
	146		3 – 19	0.07 – 5.96	0.28 – 57.09	0.0237	$6.5 \cdot 10^{-5}$	
	61	Air–HL	1– 25	0.02 – 3.40	0.10 – 24.05	0.0381	$1.2 \cdot 10^{-3}$	SL
	209	Air–Water	1	0.001–1.04	0.09 – 61.30	0.0455	0	SS
	470	Air–Oil	3 – 15	0.03 – 7.25	0.04 – 69.56	0.0502	$3.0 \cdot 10^{-5}$	SW
	131	Air–HL	3 – 22	0.03 – 7.10	0.16 – 59.52	0.0909	$1.7 \cdot 10^{-5}$	
	156		3 – 20	0.07 – 6.07	0.11 – 24.47	0.1402	$1.1 \cdot 10^{-5}$	

* Data set are identified as: SU28, SU29, SU184–187, SU199, SU24, SU25 and SU26

Table 3. Tulsa data

Source	Points	μ_L [cP]	U_{SL} [m/s]	U_{SG} [m/s]	D [m]	ϵ/D	FP
Andritsos (1986)	92	1 – 70	0.001– 0.06	4.49 – 30.09	0.0252	0	AN
	111	1 – 80	0.001– 0.19	4.29 – 29.51	0.0953		SL
							SS
							SW
Beggs (1972)	21	1	0.03 – 2.62	0.31 – 24.97	0.0254	0	AN
	22		0.02 – 1.60	0.37 – 15.12	0.0381		DB
							SL
							SS
							SW
Cheremisinoff (1977)	151	1	0.02 – 0.07	2.58 – 24.01	0.0635	0	SS
							SW
Kokal (1987)	10	8	0.03 – 0.06	1.18 – 11.51	0.0512	0	SS
	13		0.05 – 0.15	1.01 – 9.01	0.0763		SW
Mukherjee (1979)	44	1	0.03 – 3.40	0.23 – 24.06	0.0381	$3.0 \cdot 10^{-5}$	AN
							SL
							SS
							SW

A fraction of the experimental data (2060 experimental points) was used to calculate the experimental mixture friction factors. The points belonging to transition regions that come from the Cabello’s data (9 experimental points) and the Ortega’s data (32 experimental points) were excluded. The points that come from the Rivero’s data (74 experimental points), the Eaton’s data (51 experimental points) and the SU199’s data (209 experimental points) were excluded, because the pressure measurements had huge and unacceptable scatter for some points. The models and the correlations considered in section 6, including ours, are tested against the entire database (2435 experimental points).

Figure 1 shows the mixture friction factor f_M against the mixture Reynolds number Re . In this figure, two clearly defined ‘laminar and turbulent’ regions are observed, one region for values of Re less than 500 and the other one for values greater than 1000. Two reasonably good correlations were obtained fitting the data with power law correlations in both regions. However, the region between 500 and 1000 is not clearly defined.

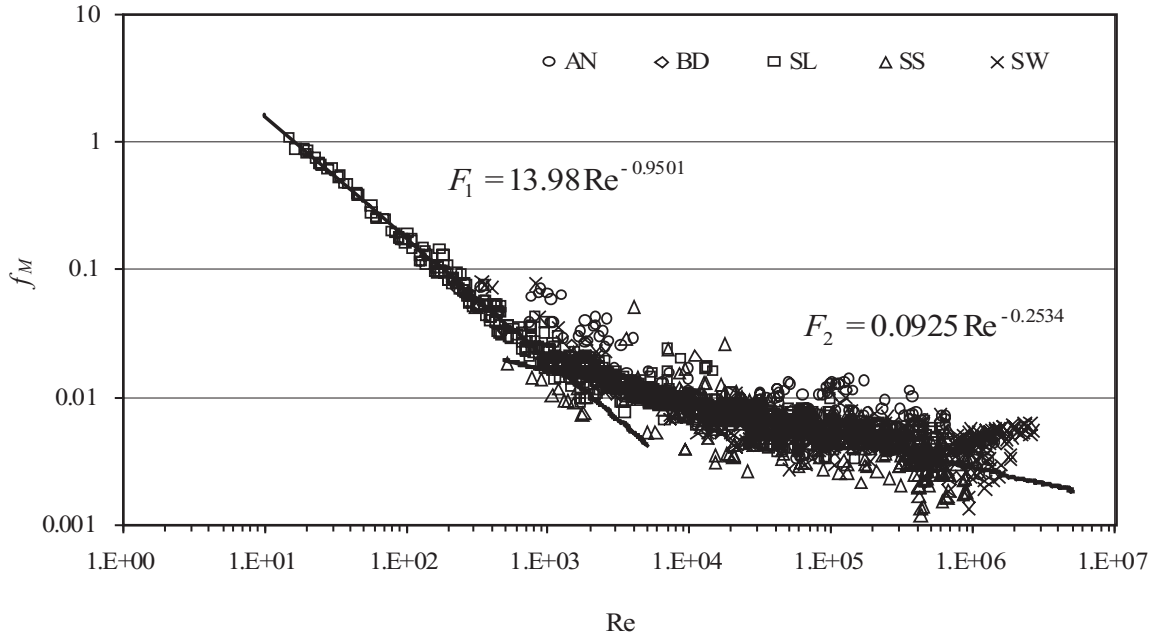


Figure 1. Power law correlations for $Re < 500$ and $Re > 1000$.

A single equation (called composite) that can be used to predict the mixture friction factors for a wide range of gas and liquid flow rates, viscosity values, and different flow patterns was obtained fitting data with a logistic dose response curve applying a technique described by Barree (Patankar *et al.*, 2002). The equation is given by

$$f_M = F_2 + \frac{(F_1 - F_2)}{\left(1 + \left(\frac{Re}{t}\right)^c\right)^d} \quad (5)$$

where F_1 and F_2 are power laws defined as

$$F_1 = a_1 Re^{b_1} \quad (6)$$

and

$$F_2 = a_2 Re^{b_2} \quad (7)$$

c, d and t, are parameters obtained fitting (5) to the 2060 data points using the non-linear optimization method of Microsoft[®] Excel Solver minimizing the residual mean square. The parameters a₁, b₁, a₂ and b₂ are obtained fitting the data with power law correlations in both regions.

Equation (5) implies that correlations in the entire range can be represented by power laws connected by transition regions (Patankar *et al.*, 2002). The parameters c, d, t, a₁, b₁, a₂, b₂ for this correlations are presented in table 4.

Table 4. Parameters of the universal composite correlation for mixture Fanning friction factor.

a ₁	b ₁	a ₂	b ₂	c	d	t
13.98	-0.9501	0.0925	-0.2534	4.864	0.1972	293

The universal composite correlation for gas–liquid Fanning friction factor (FFUC) is given by

$$f_M = 0.0925 \text{Re}^{-0.2534} + \frac{13.98 \text{Re}^{-0.9501} - 0.0925 \text{Re}^{-0.2534}}{\left(1 + \left(\frac{\text{Re}}{293}\right)^{4.864}\right)^{0.1972}} \quad (8)$$

Figure 2 shows the logistic dose response curve for the whole region.

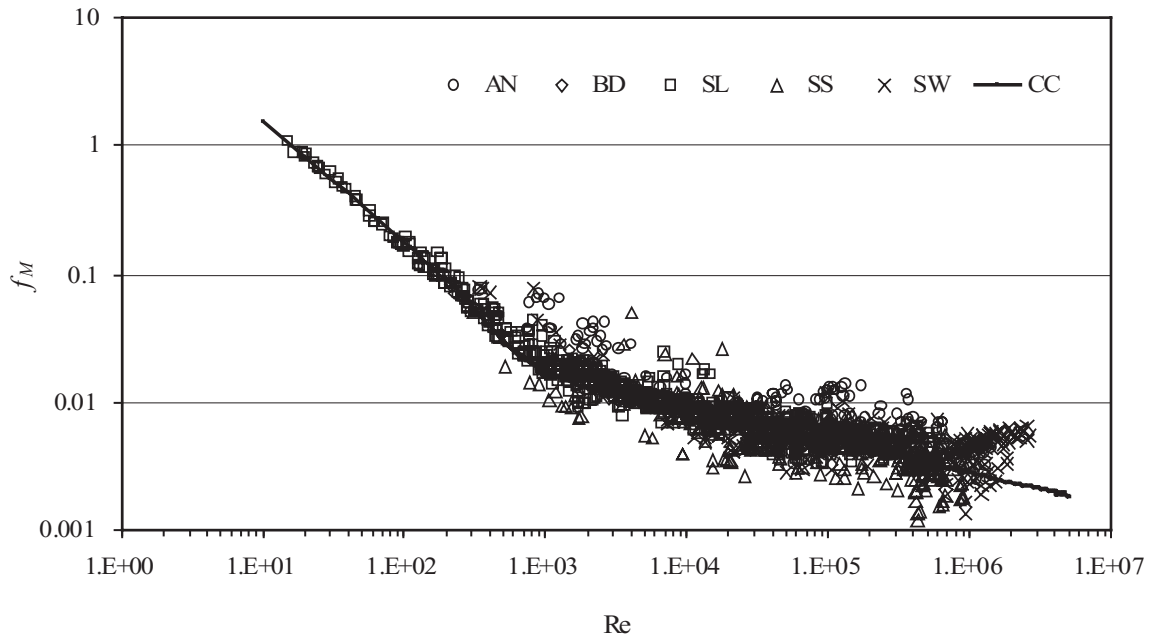


Figure 2. Universal composite correlation (8).

The standard deviation of the correlated friction factor from the measured value was estimated to be 29.05% of the measured value.

It is important to point out that most of the points for turbulent flow in figure 2 fall in a relatively narrow band even though the roughness parameters for the pipes used to collect e data in the narrow band lie in a wide band, from zero to $1.7 \cdot 10^{-3}$ (ε/D in tables 1, 2 and 3). No single-phase turbulent flow like systematic behaviour is noticed for data sets with similar relative roughness. It is possible that the disturbance due to interaction between one phase and the other could overcome the relative roughness effect in two-phase flow dynamics. The influence of relative roughness in multiphase flow needs further study, since it seems to be not completely understood.

The spread of the experimental data around the composite friction factor correlation (8) is shown in figure 3.

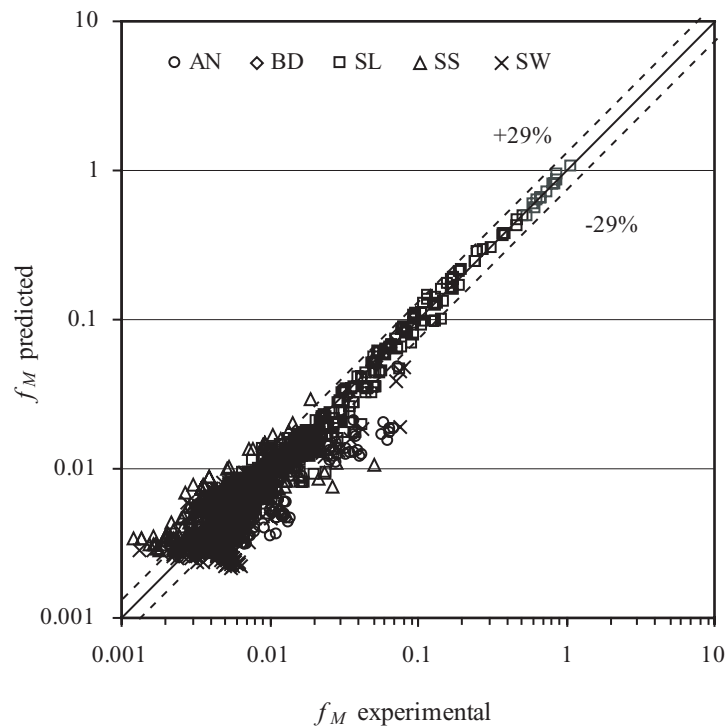


Figure 3. Predicted mixture Fanning friction factor (8) vs. experimental mixture Fanning friction factor for the universal composite correlation

The correlation (8) has an average error of -4.27% and an average absolute error of 20.27%. 75.73% of the points (1560 points) are in the band between $\pm 29\%$. The best agreements are obtained for slug and dispersed bubble flow data, with an average absolute error of 12.41% and

8.98, respectively. The worst agreements are obtained for annular and stratified flow data, with an average absolute error of 38.65% and 34.57%, respectively.

4. Friction factor correlations sorted by flow pattern (FFPC)

We fit the data from 2060 experiments to power laws using the logistic dose curve (5) fitting procedure to obtain composite correlations. Each and every experiment was classified for flow type: 1316 slug flow, 40 dispersed bubble, 528 stratified flow and 176 annular flow types and composite correlations were created for each flow type. The parameters c , d , t , a_1 , b_1 , a_2 , b_2 of each correlation are presented in table 5.

Table 5. Parameters of the gas–liquid friction factor correlations for each flow pattern

FP	a_1	b_1	a_2	b_2	c	d	t
SL	13.98	-0.9501	0.1067	-0.2629	3.577	0.2029	293
DB	13.98	-0.9501	0.1067	-0.2629	2.948	0.2236	304
ST	13.98	-0.9501	0.0445	-0.1874	9.275	0.0324	300
AN	3.671	-0.6257	0.0270	-0.1225	2.191	0.2072	10000

Figures 4 and 5 show the logistic dose response curves for slug and dispersed bubble flow, respectively.

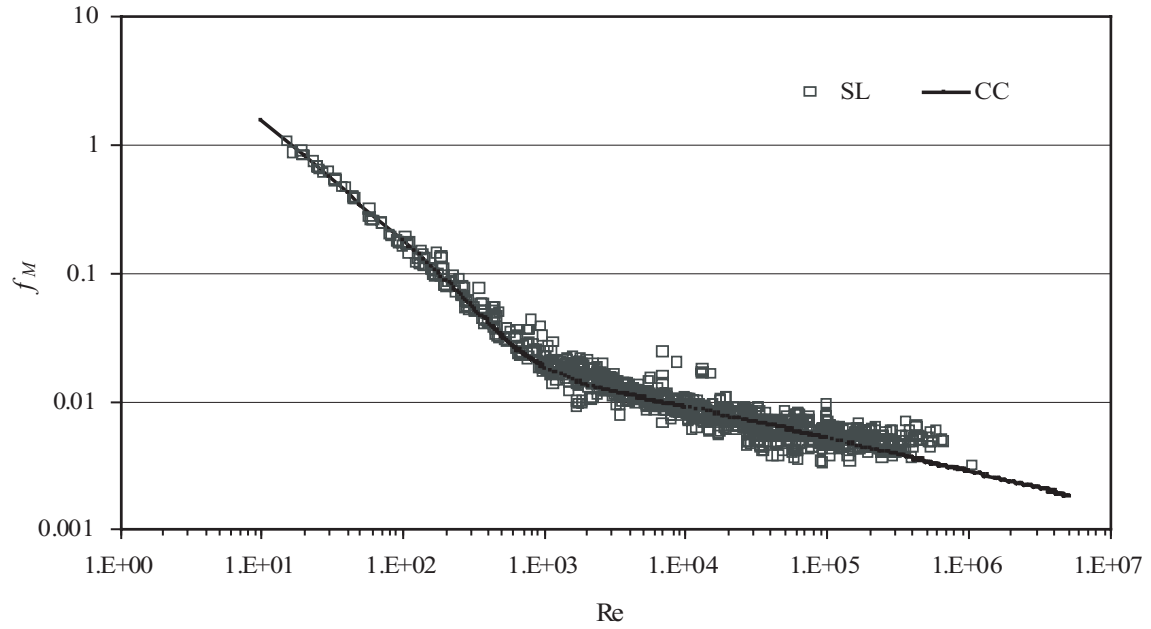


Figure 4. Composite correlation (9) for slug flow.

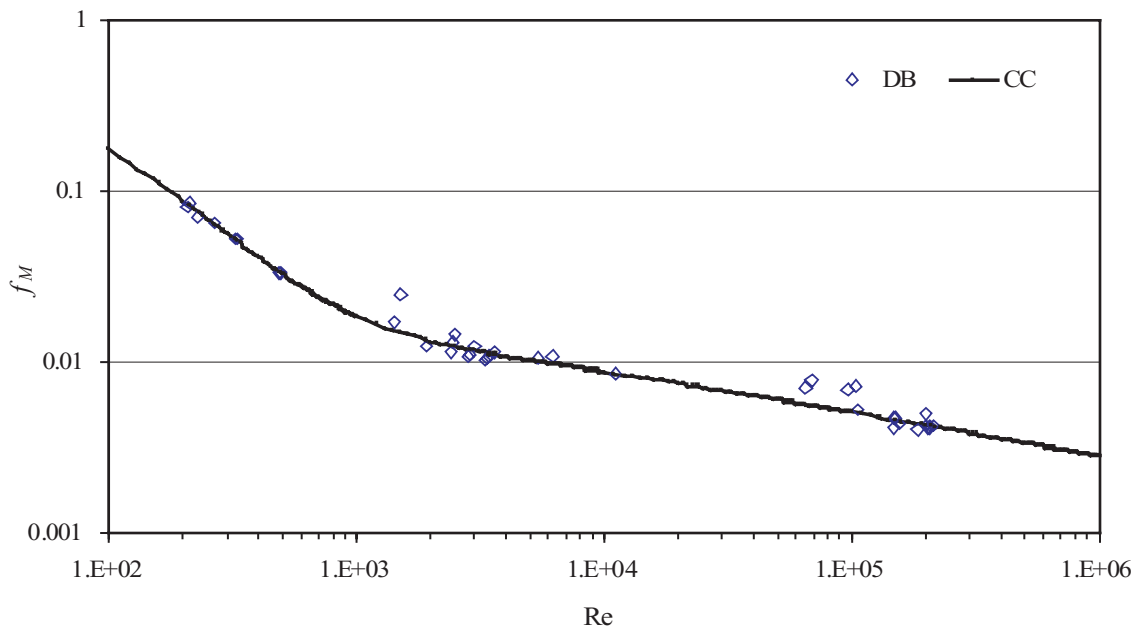


Figure 5. Composite correlation (9) for dispersed bubble flow.

The composite correlations for slug flow and dispersed bubble flow are given by, respectively:

$$f_M = 0.1067 \text{Re}^{-0.2629} + \frac{13.98 \text{Re}^{-0.9501} - 0.1067 \text{Re}^{-0.2629}}{\left(1 + \left(\frac{\text{Re}}{293}\right)^{3.577}\right)^{0.2029}} \quad (9)$$

$$f_M = 0.1067 \text{Re}^{-0.2629} + \frac{13.98 \text{Re}^{-0.9501} - 0.1067 \text{Re}^{-0.2629}}{\left(1 + \left(\frac{\text{Re}}{304}\right)^{2.948}\right)^{0.20236}} \quad (10)$$

The standard deviations for the slug and dispersed bubble flow correlations of the correlated friction factors from the measured values were estimated to be 16.61% and 12.91% of the measured values, respectively. The spread of data around the correlations for slug flow and dispersed bubble flow are shown figures 6 and 7.

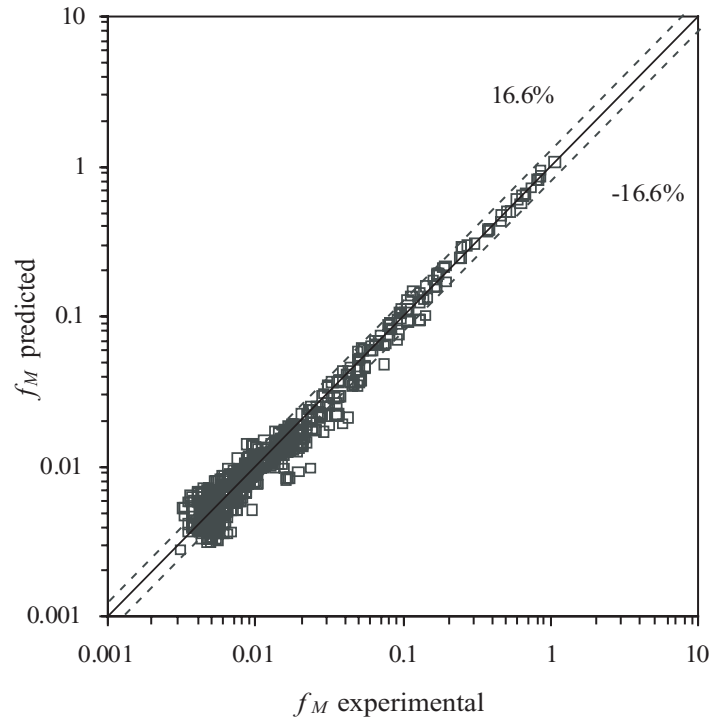


Figure 6. Predicted mixture friction factor (9) vs. experimental mixture friction factor for slug flow.

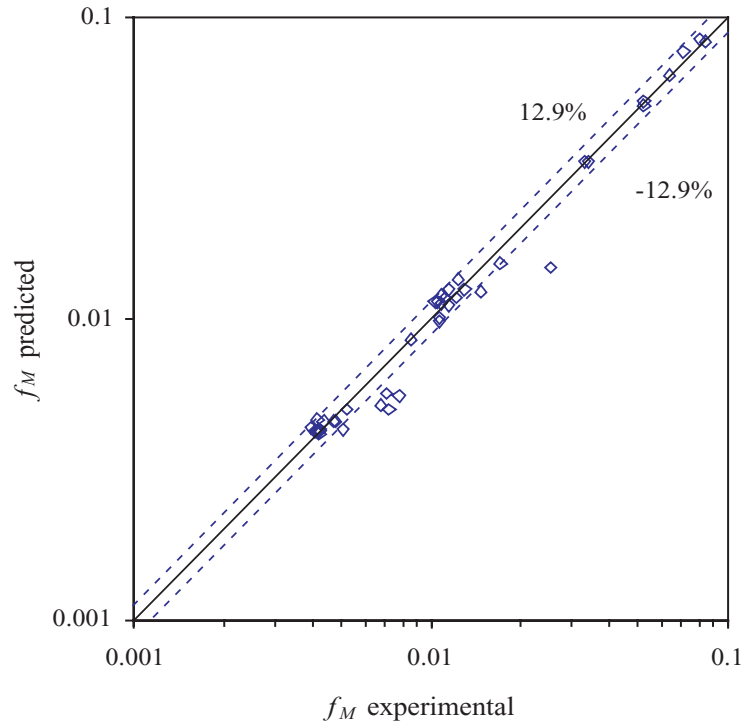


Figure 7. Predicted mixture friction factor (10) vs. experimental mixture friction factor for dispersed bubble flow

Predicted and measured values for slug flow and dispersed bubble flow are shown in figures 6 and 7; the spread of the data around predicted values is not large. The slug flow friction factor correlation has an average error of -2.17% and an average absolute error of 11.99%. 75.30% of the points (991 points) are in the band between $\pm 16.61\%$. The dispersed bubble flow friction factor correlation has an average error of -3.21% and an average absolute error of 8.32%. 82.50% of the points (33 points) are in the band between $\pm 12.91\%$.

The composite correlations for stratified and annular flow are shown in figures 8 and 9, respectively.

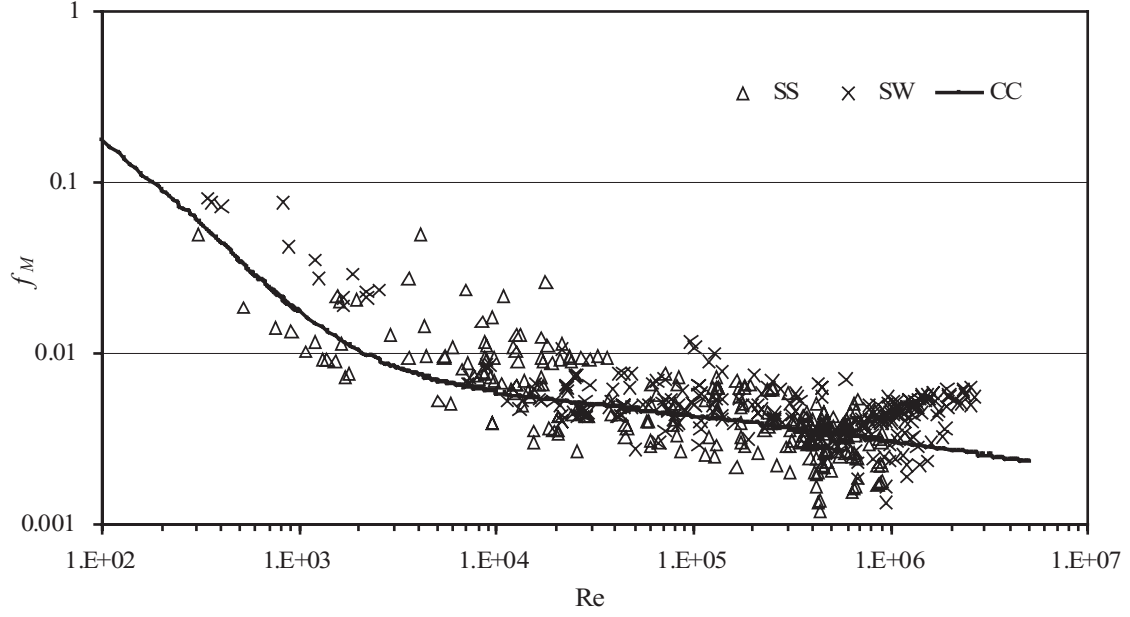


Figure 8. Composite correlation (11) for stratified flow.

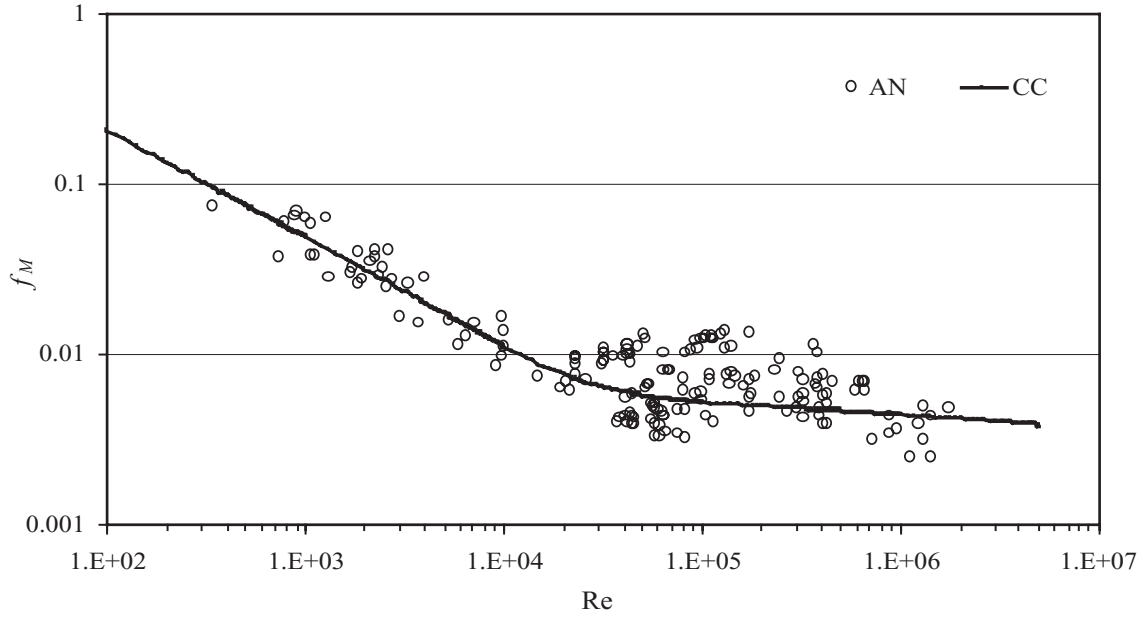


Figure 9. Composite correlation (12) for annular flow.

The composite correlations for stratified flow and annular flow are given by, respectively:

$$f_M = 0.0445 \text{Re}^{-0.1874} + \frac{13.98 \text{Re}^{-0.9501} - 0.0445 \text{Re}^{-0.1874}}{\left(1 + \left(\frac{\text{Re}}{300}\right)^{9.275}\right)^{0.0324}} \quad (11)$$

$$f_M = 0.0270 \text{Re}^{-0.1225} + \frac{3.671 \text{Re}^{-0.6257} - 0.0270 \text{Re}^{-0.1225}}{\left(1 + \left(\frac{\text{Re}}{10000}\right)^{2.191}\right)^{0.2072}} \quad (12)$$

The standard deviation of (11) for stratified flow is estimated as 38.40% of the measured value. The standard deviations (12) for annular flow is estimated to be 34.77% of the measured value. The spread of the data around the correlations for stratified and annular flow is shown in figures 10 and 11.

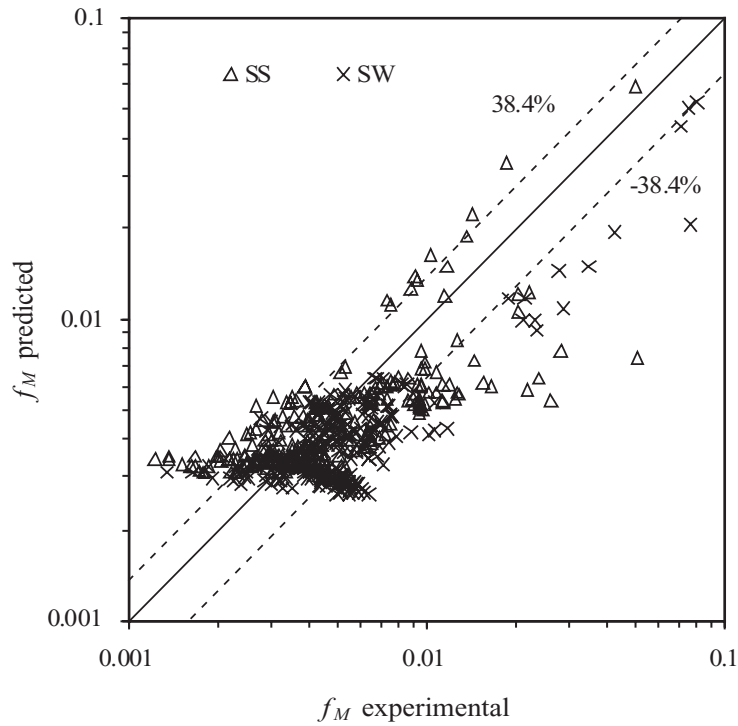


Figure 10. Predicted mixture friction factor (11) vs. experimental mixture friction factor for stratified flow.

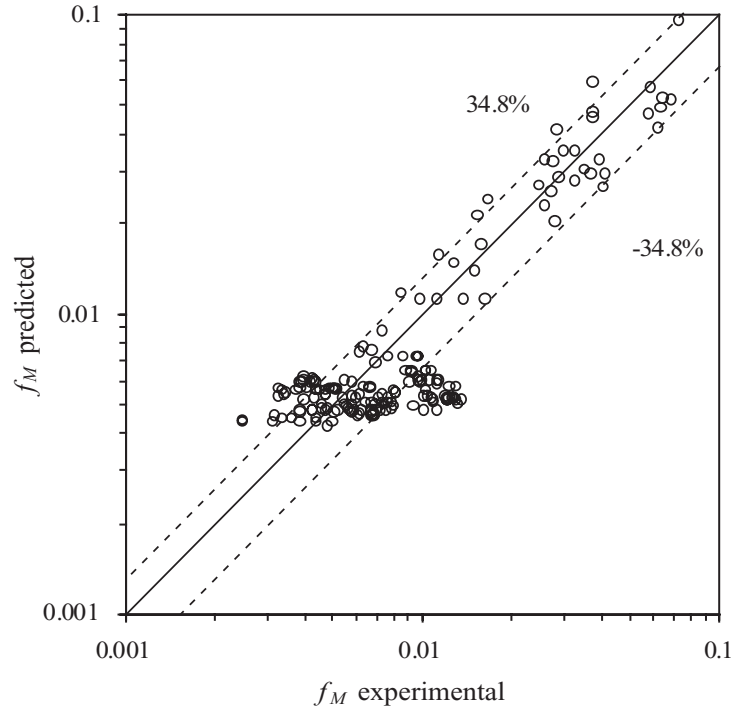


Figure 11. Predicted mixture friction factor (12) vs. experimental mixture friction factor for annular flow.

The predicted and measured values for stratified and annular flow are shown in figures 10 and 11. The average error for stratified flow is -6.80% and the average absolute error is 30.42%. Only 68.37% of the 520 points (361 points) are in the band between $\pm 38.40\%$. The average error for annular flow is -7.36% and the average absolute error of 29.59%. However, only 64.20% of the 176 points (113 points) are in the band between $\pm 34.77\%$.

5. Performance comparison of correlations and models for pressures drop from various sources against the data from 2435 experiments

The performance of predictions for the pressure drop in the 2435 experiments in our database from the literature and our correlations will now be considered. Sources for the predictions are indexed as follows:

- DUC (Dukler *et al.*, 1964),
- BBC (Beggs and Brill, 1973),
- XMM (Xiao *et al.*, 1990),
- OMM (Ouyang, 1998),
- OHM (Ouyang, 1998),

ORC (Ortega *et al.*, 2001),

PMM (Padrino *et al.*, 2002),

FFPC (Friction factor flow pattern correlations from equations (9), (10), (11) and (12)),

FFUC (Friction factor universal correlation from equation (8)),

The last C in the acronym stands for correlation, the MM stands for mechanistic model and HM stands for homogeneous model.

The correlations developed in previous sections leading to FFPC and FFUC were developed by processing 2060 points. The remaining 375 data points which were omitted in forming the correlations were also classified for flow pattern so that those data points could be compared with predictors that specify flow type.

The comparison of the predictions of $\Delta p/L$ from different sources was accomplished by using a weighted measure PF which is a modification of a measure recommended by Ansari *et al.* (1994) defined by

$$PF = \frac{|E_1| - |E_{1\min}|}{|E_{1\max}| - |E_{1\min}|} + \frac{E_2 - E_{2\min}}{E_{2\max} - E_{2\min}} + \frac{E_3 - E_{3\min}}{E_{3\max} - E_{3\min}} + \frac{|E_4| - |E_{4\min}|}{|E_{4\max}| - |E_{4\min}|} + \frac{E_5 - E_{5\min}}{E_{5\max} - E_{5\min}} + \frac{E_6 - E_{6\min}}{E_{6\max} - E_{6\min}} \quad (13)$$

where E_1 is the average percent error, E_2 is average absolute percent error, E_3 is the standard deviation of the correlated value from the experimental value divided by the experimental value (root mean square percent error), E_4 is the average error, E_5 is average absolute error, E_6 is the standard deviation of the correlated value from the experimental value (root mean square error) which are defined as

$$E_1 = \left[\frac{1}{n} \sum_{i=1}^n \frac{(\Delta p_i / L)_{pred} - (\Delta p_i / L)_{exp e}}{(\Delta p_i / L)_{exp e}} \right] * 100 \quad (14)$$

$$E_2 = \left[\frac{1}{n} \sum_{i=1}^n \left| \frac{(\Delta p_i / L)_{pred} - (\Delta p_i / L)_{exp e}}{(\Delta p_i / L)_{exp e}} \right| \right] * 100 \quad (15)$$

$$E_3 = \left[\sqrt{\frac{1}{n-1} \sum_{i=1}^n \left(\frac{(\Delta p_i / L)_{pred} - (\Delta p_i / L)_{exp e}}{(\Delta p_i / L)_{exp e}} \right)^2} \right] * 100 \quad (16)$$

$$E_4 = \frac{1}{n} \sum_{i=1}^n (\Delta p_i / L)_{pred} - (\Delta p_i / L)_{exp e} \quad (17)$$

$$E_5 = \frac{1}{n} \sum_{i=1}^n |(\Delta p_i / L)_{pred} - (\Delta p_i / L)_{exp e}| \quad (18)$$

$$E_6 = \left[\sqrt{\frac{1}{n-1} \sum_{i=1}^n \left((\Delta p_i / L)_{pred} - (\Delta p_i / L)_{exp e} \right)^2} \right] \quad (19)$$

The average percent error is a measure of the agreement between predicted and measured data. It indicates the degree of over-prediction (positive values) or under-prediction (negative values). Similarly, the average absolute percent error is a measure of the agreement between predicted and measured data. However, in this parameter the positive errors and the negative errors are not canceled. For this reason, the average absolute percent error is considered a key parameter in order to evaluate the prediction capability of a correlation. The standard deviation indicates how close the predictions are to the experimental data. The statistical parameters E_4 , E_5 and E_6 are similar to E_1 , E_2 and E_3 but the difference is that they are not based on the errors relative to the experimental pressure drop per unit length.

The minimum and maximum possible values for the PF are 0 and 6, corresponding to the best and the worst prediction performance, respectively.

The comparison of the accuracy of pressure gradient prediction of the correlations and the models from different authors against 2435 points is shown in table 6. The measure of performance (PF) is a weighed measure using data from the columns E_1 through E_6 . The overall performance is given in the column PF, the smaller the number the more accurate is the prediction. The statistical parameters E_1 , E_2 , E_3 , E_4 , E_5 and E_6 for each correlation or model are included.

Table 6. Comparison of the accuracy of pressure gradient prediction of the correlations and the models from different authors against 2435 points.

Model or Correlation	PF	Statistical Parameters					
		E_1 [%]	E_2 [%]	E_3 [%]	E_4 [Pa/m]	E_5 [Pa/m]	E_6 [Pa/m]
<i>FFPC</i>	0.02	-4.88	21.71	43.17	-72.58	316.11	805.05
<i>FFUC</i>	0.15	-5.78	24.61	46.76	-167.05	355.84	905.58
<i>DUC</i>	0.18	-6.86	24.85	58.03	-61.34	401.60	1025.78
<i>PMM</i>	0.32	-16.89	28.12	44.53	31.04	492.53	1232.89
<i>XMM</i>	0.57	5.80	39.94	111.66	-139.94	474.20	1063.25
<i>OHM</i>	0.57	-25.39	33.39	50.96	-266.56	438.04	1128.86
<i>ORC</i>	2.05	66.51	78.15	148.87	459.75	672.36	2374.55
<i>OMM</i>	3.22	95.74	137.33	326.82	-234.27	483.01	958.99
<i>BBC</i>	4.52	57.85	64.61	204.12	1893.18	1983.48	23631.94

The performance of our correlation (9), (10), (11) and (12) sorted by flow pattern FFPC is best and the universal correlation FFUC given by (8) in which flow patterns are ignored is second best.

It is of interest for applications to pipelines in reservoirs of heavy oil to evaluate predictors against high viscosity ($\mu_L \geq 400$ cP) data; this is done in table 7.

Table 7. Comparison of the accuracy of pressure gradient prediction of the correlations and the models from different authors against high viscosity data ($\mu_L \geq 400$ cP)

Model or Correlation	PF	Statistical Parameters					
		E_1 [%]	E_2 [%]	E_3 [%]	E_4 [Pa/m]	E_5 [Pa/m]	E_6 [Pa/m]
<i>FFPC</i>	0.30	-7.69	13.85	19.50	-324.70	548.52	1002.14
<i>ORC</i>	2.03	-15.66	17.06	23.71	-784.29	806.16	1558.81
<i>PMM</i>	2.89	-5.54	25.50	38.62	-67.51	1209.06	2098.29
<i>XMM</i>	2.98	-14.60	21.90	35.38	-774.55	919.34	1800.90
<i>FFUC</i>	3.19	-17.83	22.21	32.37	-839.13	990.39	1877.80
<i>BBC</i>	3.71	8.38	32.16	36.59	409.69	1431.56	1991.89
<i>OMM</i>	4.47	-24.84	25.70	37.79	-1139.83	1160.54	2133.75
<i>OHM</i>	4.55	-25.33	26.13	38.20	-1148.14	1168.21	2139.71
<i>DUC</i>	5.82	-33.28	34.32	45.78	-1215.72	1275.54	2299.17

The correlation FFPC which have been sorted by flow type again have the best performance, but the universal correlation fall to fifth place. As a practical matter, the flow of heavy oils in pipelines in reservoirs of heavy oil will be much slower than the flows of mobile of gas in mobile liquids like water. Turbulent flow, which leads to dispersed bubbles and annular flow, do not typically occur in high viscosity fluids.

We turn now to an evaluation of the predictors when the experimental data is restricted by flow type. The following data were used: 1416 slug flow data points, 40 dispersed bubble data points, 689 stratified flow data points, and 249 annular flow data points. 41 data points corresponding to transitions were not considered in this evaluation. The PF and the statistical parameters for each flow patterns are presented in tables 8 – 11. This kind of comparison naturally favors correlations like FFPC which recognize the flow pattern. The excellent performance of FFUC, which does not recognize the flow pattern is noteworthy. For viscous oils, slug flow and universal correlations may be recommended. The universal correlation also works well in the flow types of dispersed bubble and annular flow which are generated by turbulence.

Table 8. Evaluation of the correlations and the models using slug flow data.

Model or Correlation	PF	Statistical Parameters					
		E_1 [%]	E_2 [%]	E_3 [%]	E_4 [Pa/m]	E_5 [Pa/m]	E_6 [Pa/m]
FFPC	0.01	-2.46	12.97	18.33	-64.40	356.30	806.01
FFUC	0.17	-4.71	13.34	18.48	-137.43	363.97	827.89
DUC	0.67	-2.55	18.23	29.67	98.13	456.02	1058.43
OHM	0.73	-10.81	16.73	23.77	-224.93	423.60	818.90
PMM	0.89	-4.90	17.64	24.90	245.20	566.03	1338.74
OMM	1.17	-16.14	20.56	27.25	-297.20	427.74	757.83
XMM	1.43	-8.76	21.05	42.94	-238.29	513.36	1052.57
ORC	1.99	10.67	22.72	41.60	428.59	644.56	1796.58
BBC	6.00	33.94	37.23	62.40	1499.12	1526.97	4194.43

Table 9. Evaluation of the correlations and the models using dispersed bubble flow data

Model or Correlation	PF	Statistical Parameters					
		E_1 [%]	E_2 [%]	E_3 [%]	E_4 [Pa/m]	E_5 [Pa/m]	E_6 [Pa/m]
FFPC	0.34	-3.37	8.30	12.56	-144.79	268.42	558.73
DUC	0.43	-2.31	10.88	15.88	-22.77	267.14	430.77
FFUC	0.69	-4.57	8.99	13.22	-187.76	318.66	608.44
ORC	1.48	-9.56	9.94	15.99	-328.58	338.39	638.78
PMM	1.74	-4.97	12.34	17.04	94.60	528.37	898.92
OHM	1.90	-10.49	11.06	16.14	-388.11	396.46	743.57
OMM	1.92	-10.53	11.17	16.25	-388.51	397.38	743.75
XMM	4.32	-19.66	19.69	25.28	-562.37	566.07	863.44
BBC	5.80	16.11	21.89	26.40	829.93	913.49	1425.16

Table 10. Evaluation of the correlations and the models using stratified flow data.

Model or Correlation	PF	Statistical Parameters					
		E_1 [%]	E_2 [%]	E_3 [%]	E_4 [Pa/m]	E_5 [Pa/m]	E_6 [Pa/m]
FFUC	0.05	2.62	42.26	78.62	-28.04	65.24	169.81
FFPC	0.17	-7.06	37.73	73.78	-42.75	63.59	184.64
DUC	0.41	-6.91	36.22	97.13	-53.81	73.97	221.44
PMM	0.50	-30.75	41.34	66.60	-63.80	78.27	212.20
OHM	0.76	-42.72	56.81	77.77	-83.33	89.73	203.98
XMM	1.42	18.56	62.27	163.87	65.31	129.15	415.84
BBC	2.57	86.93	98.53	155.14	120.56	149.97	591.11
ORC	3.53	175.05	185.76	260.63	177.07	207.82	445.12
OMM	5.57	375.68	408.47	607.19	167.69	285.88	438.02

Table 11. Evaluation of the correlations and the models using annular flow data.

Model or Correlation	PF	Statistical Parameters					
		E_1 [%]	E_2 [%]	E_3 [%]	E_4 [Pa/m]	E_5 [Pa/m]	E_6 [Pa/m]
FFPC	0.05	-10.95	29.60	33.95	-92.04	712.72	1476.08
DUC	0.32	-27.89	32.02	38.61	-830.31	903.96	1753.62
FFUC	0.48	-33.33	43.01	47.20	-621.68	1031.67	1899.61
PMM	0.81	-52.37	54.09	58.04	-1041.83	1121.24	1983.01
OMM	0.92	-6.06	90.20	145.26	-849.44	1280.14	2163.31
OHM	1.08	-63.01	68.26	72.79	-882.19	1401.13	2832.41
XMM	1.38	61.07	92.47	192.75	-5.03	1161.30	1981.09
ORC	2.23	108.83	115.76	137.80	1727.84	2127.30	5987.36
BBC	6.00	126.90	139.72	565.21	9398.50	9973.73	73340.33

6. Summary and Conclusions

Data from 2435 gas–liquid flow experiments in horizontal pipelines were sorted by flow pattern and a data structure suitable for the construction of correlations of friction factor vs. Reynolds number was created.

A mixture friction factor (1) and mixture Reynolds number (4) were selected to reduce the scatter of the data. The Reynolds number is based on the mixture velocity and the liquid kinematic viscosity; the frictional resistance of the liquid is most important.

Data from 2060 of the 2435 experiments were processed for power law correlation in log–log plots of friction factor vs. Reynolds number.

Power laws for laminar and turbulent gas–liquid flow were determined for all the 2060 points irrespective of flow patterns; we called such correlations which are independent of flow type universal.

Power laws for laminar and turbulent gas–liquid flow were determined for subsets of the 2060 points corresponding to stratified, slug, disperse bubble and annular flow.

The transition region going from laminar to turbulent flow was fit to a logistic dose curve. This fitting procedure leads rational fractions of power laws which reduce to laminar flow at small Reynolds number and to turbulent flow at large Reynolds number. We call these rational fraction of power laws composite; one formula for all Reynolds number. Composite power laws are very practical because the transition region is predicted to a statistical accuracy consistent with spread of the data.

The predictions of the composite correlations were tested internally for the spread of the actual data against the predictions from 2060. The same tests were carried out for the correlations sorted by flow type. The standard deviations are small for slug flow, which is main flow type of viscous oils, and bubble flow which requires turbulent flow with a relatively small gas fraction.

The prediction of the composite correlations were tested externally against correlations and mechanistic models in the literature. The composite correlations sorted by flow type are more accurate than any other predictor for all cases except stratified flow which the universal composite correlation is the most accurate. The universal composite correlation is second best in the data set in which all flow types are included followed in third place by the Dukler *et al.* (1964) correlation. When sorted by viscosity, the Dukler correlation is the worst. Slug flow is the

main flow type in the data set for high viscosity liquid (42.74% points) and the composite correlation for slug flow may be recommended.

In annular and stratified flow the effect of the relative velocity of the phases, neglected in this paper, should be significant. Including the holdup, as was done by Mata *et al.* (2002) could give rise to improved correlations.

Universal (independent of flow type) and composite (for all Reynolds numbers) correlations are very useful for field operations for which the flow type may not be known. It is best guess for the pressure gradient when the flow type is unknown or different flow types are encountered in one line.

A dimensionless pipe roughness is given in the data base and ranges from smooth (41% points) to rough (59% points) pipes. The data and correlations for two-phase turbulent flow in pipes do not appear to depend strongly on roughness; it may be dominated by natural fluctuation of one phase by other. This needs further study.

7. Acknowledgments

The authors would like to thank to A. Brito and J. Colmenares for their contributions in the Intevep's data collection. F. Garcia would like to acknowledge the CDCH-UCV, Escuela de Ingeniería Mecánica de la Universidad Central de Venezuela and PDVSA-Intevep for supporting his Doctoral Study. The work of D.D. Joseph was supported by the PDVSA-Intevep and the Engineering Research Program of the Office of Basic Energy Sciences at the DOE, and under an NSF/GOALI grant from the division of Chemical Transport Systems.

8. References

- Agrawal, S.S., 1971. Horizontal Two Phase Stratified Flow in Pipe M.Sc. Thesis, Univ. of Calgary.
- Alves, G.E., 1954. Concurrent Liquid–Gas Flow in a Pipe–Line Contactor, *Chemical Engineering Progress*, 50 (9), pp. 449–456.
- Andritsos, N., 1986. Effect of Pipe Diameter and Liquid Viscosity on Horizontal Stratified Flow, Ph.D. Dissertation, U. of Illinois at Champaign–Urbana.
- Ansari, A. M., Sylvester, N. D., Sarica, C., Shoham, O., Brill, J. P., 1994. A Comprehensive Mechanistic Model for Upward Two–Phase Flow in Wellbores, *SPE Production & Facilities J.*, May, pp. 142–152.
- Aziz, K., Gregory, G.A., Nicholson, M., 1974. Some observation on the Motion of Elongated Bubbles in Horizontal Pipes, *Canadian Journal of Chemical Engineering*, 52, pp. 695–702.
- Beggs, H. D., 1972. An Experimental Study of Two–Phase Flow in Inclined Pipes, Ph.D. Dissertation, U. of Tulsa.
- Beggs, H. D., Brill, J. P., 1973. A Study of Two Phase Flow in Inclined Pipes, *J. of Petroleum Technology*, 25(5), pp. 607–617.
- Cabello, R., Cárdenas, C., Lombano, G., Ortega, P., Brito, A., Trallero, J., Colmenares, J., 2001. Pruebas Experimentales con Kerosén/Aire para el Estudio de Flujo Tapón con Sensores Capacitivos en una Tubería Horizontal, INT–8898,2001. PDVSA INTEVEP, 50 p.
- Cheremisinoff, N. P., 1977. An Experimental and Theoretical Investigation of Horizontal Stratified and Annular Two Phase Flow with Heat Transfer, Ph.D. Dissertation, Clarkson College of Technology.
- Dukler, A.E., Wicks III, M., Cleveland, R.G., 1964. Frictional Pressure Drop in Two–Phase Flow: B. An Approach through Similarity Analysis, *AIChE Journal*, Vol. 10, January, pp. 44–51.
- Eaton, B.A., 1966. The Prediction of Flow Patterns, Liquid Holdup and Pressure Losses Occurring During Continuous Two–Phase Flow in Horizontal Pipelines. Ph.D. Thesis, University of Texas, 169 p.
- Govier, G.W., Omer, M.M., 1962. The Horizontal Pipeline Flow of Air–Water Mixture, *Canadian Journal of Chemical Engineering*, 40, pp. 93.
- Joseph, D. D., 2001. Power law correlations for lift from direct numerical simulation of solid–liquid flow, *Int. J. Multiphase Fluids*, accepted 2001.
- Kokal, S. L., 1987. An Experimental Study of Two–Phase Flow in Inclined Pipes, Ph.D. Dissertation, U. of Calgary, Alberta, Canada.
- Mata, C., Vielma, J., Joseph, D., 2002. Power law correlations for gas/liquid flow in a flexible pipeline simulating terrain variation, *Int. J. Multiphase Flow*, submitted.
- Mattar, L., 1973. Slug Flow Uphill in an Inclined Pipe, M.Sc. Thesis, University of Calgary.
- Mukherjee, H., 1979. An Experimental study of Inclined Two–Phase Flow, Ph.D. Dissertation, U. of Tulsa.
- Ortega, P., Trallero, J., Colmenares, J., Brito, A., Cabello, R., González, P., 2001. Experimentos y Validación de Modelo para Predicción del Gradiente de Presión de Flujo Tapón en Tuberías Horizontales para un Sistema Bifásico altamente Viscoso aceite (1200 cP)/aire, INT–8879,2001. PDVSA INTEVEP, 37 p.

- Ortega, P., Trallero, J., Colmenares, J., Cabello, R., González, P., 2000. Modelo para la Predicción de la Caída de Presión en Flujo Tapón para una Tubería Horizontal. INT-8123,2000. PDVSA INTEVEP, 19 p.
- Ouyang, L. B., 1998. Single Phase and Multiphase Fluid Flow in Horizontal Wells, Ph.D. Dissertation Thesis. Department of Petroleum Engineering. School of Earth Sciences. Stanford University. Stanford, CA. 248 p.
- Padrino, J., Pereyra, E., Brito, A., Garcia, F., Cardozo, M., Ortega, P., Colmenares, J., Trallero, J., 2002. Modelo para la predicción del Gradiente de Presión en Pozos y Tuberías Horizontales – Parte I, INT-9508,2002. PDVSA INTEVEP, 141 p.
- Pan, T. W., Joseph, D. D., Bai, R., Glowinski, R., Sarin, V., 2002. Fluidization of 1204 spheres: simulation and experiment, *J. Fluid Mech.*, 451, pp.169–191.
- Patankar, N. A., Huang, P. Y., Ko, T., Joseph D. D., 2001a. Lift-off of a single particle in Newtonian and viscoelastic fluids by direct numerical simulation, *J. Fluid Mech.*, 438, pp. 67–100.
- Patankar, N. A., Ko, T., Choi, H. G., Joseph, D. D., 2001b. A correlation for the lift-off of many particles in plane Poiseuille flows of Newtonian fluids, *J. Fluid Mech.*, 445, pp. 55–76.
- Patankar, N.A., Joseph, D.D., Wang, J., Barree, R., Conway, M., and Asadi, M., 2002. Power Law Correlations for Sediment Transport in Pressure Driven Channel Flows, *Int. J. Multiphase Flow*, 28(8), pp. 1269–1292.
- Pereyra, E., Ortega, P., Trallero, J., Colmenares, J., 2001. Validación del Modelo Mecanicista de Gradiente de Presión para Flujo Tapón en un Sistema Crudo/Gas, INT-8894,2001. PDVSA INTEVEP, 48p.
- Rivero, M., Laya, A., and Ocando, D., 1995. Experimental Study on the Stratified–Slug Transition for Gas–Viscous Liquid Flow in Horizontal Pipelines, *BHR Group Conf. Ser. Publ.*, 14(95), pp. 293–304.
- Viana, F., Pardo, R., Yáñez, R., Trallero, J., 2001. Universal Correlation for the Rise Velocity of Taylor Bubbles in Round Pipes, *Int. J. Multiphase Flow*, submitted.
- Wang, J., Joseph, D. D., Patankar, N. A., Conway, M., Barree, B., 2002. Bi–power law correlations for sedimentation transport in pressure driven channel flows, *Int. J. Multiphase Flow*, submitted. (NSF–GOALI)
- Xiao, J. J., Shoham, O., Brill, J. P., 1990. A Comprehensive Mechanistic Model for Two–Phase Flow in Pipelines, In *The 65th SPE Annual Technical Conference and Exhibition*, New Orleans, LA. Paper SPE 20631. pp. 167–180. September 23 – 26.
- Yu, C., 1972. Horizontal Flow of Air–Oil Mixtures in the Elongated Bubble Flow Pattern. M.Sc. Thesis, University of Calgary.

9. Nomenclature

a : power-law's parameter
 b : power-law's parameter
 c : correlation's parameter
 d : correlation's parameter
 D : diameter [m]
 E : statistical parameters
 F : power laws of the logistic dose curve
 f : Fanning friction factor
 L : pipe length [m]
 p : pressure [Pa]
 Δp : pressure drop [Pa]
 Q : volumetric flow rate [m³/s]
 Re : Reynolds number
 t : correlation's parameter
 U : velocity [m/s]

Greek symbols

ε : absolute pipe roughness [m]
 λ_L : liquid flow rate fraction
 μ : dynamic viscosity [Pa.s]
 ν : kinematic viscosity [m²/s]
 ρ : density [kg/s]
 σ : standard deviation
 τ : Shear stress [N/m³]

Subscripts:

FP : flow pattern
 G : gas
 L : liquid

max : maximum
 min : minimum
 M : mixture
 SG : superficial gas
 SL : superficial liquid
 W : wall

Abbreviations:

AN : annular flow
 BBC : Beggs and Brill correlation
 CC : composite correlation
 DB : dispersed bubble flow
 DUC : Dukler correlation
 $FFUC$: friction factor universal correlation
 $FFPC$: friction factor correlations per flow pattern
 FP : flow patterns
 HL : hydrocarbon Liquid
 PF : modified relative performance factor
 OHM : Ouyang homogeneous model
 OMM : Ouyang mechanistic model
 ORC : Ortega correlation
 PMM : Padrino mechanistic model
 SL : slug flow
 SS : stratified smooth flow
 ST : stratified flow
 SW : stratified wavy flow
 XMM : Xiao mechanistic model

List of figures

Figure 1. Power law correlations for $Re < 500$ and $Re > 1000$.

Figure 2. Universal composite correlation (8).

Figure 3. Predicted mixture Fanning friction factor (8) vs. experimental mixture Fanning friction factor for the universal composite correlation.

Figure 4. Composite correlation (9) for slug flow.

Figure 5. Composite correlation (9) for dispersed bubble flow.

Figure 6. Predicted mixture friction factor (9) vs. experimental mixture friction factor for slug flow.

Figure 7. Predicted mixture friction factor (10) vs. experimental mixture friction factor for dispersed bubble flow.

Figure 8. Composite correlation (11) for stratified flow.

Figure 9. Composite correlation (12) for annular flow.

Figure 10. Predicted mixture friction factor (11) vs. experimental mixture friction factor for stratified flow.

Figure 11. Predicted mixture friction factor (12) vs. experimental mixture friction factor for annular flow.